HHS Public Access

Author manuscript

J Biol Chem. Author manuscript; available in PMC 2016 February 22.

Published in final edited form as:

J Biol Chem. 2004 June 4; 279(23): 24197–24202. doi:10.1074/jbc.M402452200.

Structural and Ligand Recognition Characteristics of an Acetylcholine-binding Protein from *Aplysia californica*[*]

Scott B. Hansen[‡,§], **Todd T. Talley**[‡], **Zoran Radić**[‡], and **Palmer Taylor**[‡,¶]

[‡]Department of Pharmacology, University of California, San Diego, La Jolla, California 92093-0636

[§]Department of Chemistry and Biochemistry, University of California, San Diego, La Jolla, California 92093-0636

Abstract

We generated an acetylcholine-binding protein from *Aplysia californica* by synthesis of a cDNA found in existing data bases and its expression in mammalian cell culture. Its subunit assembly and ligand recognition behavior were compared with the binding protein previously derived from *Lymnaea stagnalis*. The secreted proteins were purified by elution from columns of attached antibodies directed to the FLAG epitope encoded in the expression construct. Although the sequences of the two proteins from marine and fresh water mollusks exhibit the characteristic features of the extracellular domain of the nicotinic receptor, they only possess 33% amino acid identity. Both assemble as stable pentamers with five binding sites per pentamer, yet they show distinguishing features of stability and sensitivity to epitope tag placement. Both proteins exhibit changes in tryptophan fluorescence upon ligand binding; however, the magnitude of the changes differs greatly. Moreover, certain ligands show marked differences in dissociation constants for the two proteins and can be regarded as distinguishing or signature ligands. Hence, the two soluble proteins from mollusks, which can be studied by a variety of physical methods, become discrete surrogate proteins for the extracellular domains of distinct subtypes of nicotinic acetylcholine receptors.

Nicotinic acetylcholine receptors are prototype molecules for the large superfamily of pentameric ligand-gated ion channels (1–3). Due to their abundance in the electric organs of *Torpedo* sp. and the finding that peptide toxins from elapid venoms bind with high affinity to the receptor (4, 5), the acetylcholine receptor became the first neurotransmitter receptor to be characterized as a molecular entity (6). The receptor from *Torpedo*, similar to the receptor found in skeletal muscle throughout the fish and mammal phyla, assembles as a pentamer composed of four distinct subunits with only one of the subunits being expressed as two copies. The two binding sites, which in the muscle receptor are not identical in recognition characteristics, reside at the interface of the α and its partnering subunits. At least 12 nicotinic receptor subunits from mammalian neuronal tissues have been isolated,

[*]This work was supported by United States Public Health Service Grants R37-GM18360 (to P. T.) and GM 07752, a Tobacco-related Disease Program fellowship (to S. B. H.), and fellowship GM NS043063 (to T. T. T.).

[¶]To whom correspondence should be addressed. Tel.: 858-534-1366; Fax: 858-534-8248.

and they assemble in selected permutations of α and β subtypes. The simplest subtypes structurally are the homomeric pentamers of α subunits such as those from the α7 subtype (1, 7).

To function as gated channels, the receptor protein must span the membrane multiple times. The four transmembrane spans on each of the five subunits create a substantial region of hydrophobicity that precludes facile crystallization of this protein. Recent electron microscopy reconstruction analysis has led to a structure of the transmembrane region resolved to 4 Å and a description of the extracellular domain at somewhat lower resolution (8). An additional specialization of nature has led investigators to a high resolution structure of the extracellular domain of the receptor. The fresh water snail, *Lymnaea stagnalis*, produces a soluble protein, termed the acetylcholine-binding protein (AChBP)[1] that binds acetylcholine (9, 10). Characterization of its ligand recognition characteristics shows similar ligand specificity to the nicotinic acetylcholine receptor (10, 11). The *Lymnaea* binding protein is also pentameric and is composed of identical subunits, most closely resembling the extracellular domain of the α7 receptor found in neurons.

Recently, we constructed a cDNA encoding the *Lymnaea* AChBP by ligating a series of chemically synthesized oligonucleotides into an expression construct. The encoded protein was expressed to study its ligand recognition properties and structure in solution (11). Other potential sequences of candidate AChBPs exist in data bases of invertebrate species. Herein, we describe the expression and properties of a distinct binding protein from a salt water mollusk, *Aplysia californica*. Although its sequence shares the hallmark features characteristic of the *Lymnaea* protein as well as the nicotinic receptor itself, the two binding proteins come from evolutionary distant species and show only 33% amino acid residue identity. Upon purification, the *Aplysia* protein revealed structural and ligand recognition properties distinct from the *Lymnaea* protein, enabling us to analyze comparatively two subtypes of binding proteins.

MATERIALS AND METHODS

Construction of an Expression Vector cDNA

The cDNA encoding the *A*-AChBP was synthesized using the nucleotide coding sequence found in an *Aplysia* data base. Briefly, oligonucleotides extending up to 100 bp and containing triplet codons with frequent mammalian codon usage (12) were ligated into a p3×FLAG-CMV-9 expression vector (Sigma) containing a preprotrypsin leader peptide followed by an N-terminal 3× FLAG epitope and a C-terminal His_6 tag. Three alternative expression plasmids were synthesized and compared with the corresponding plasmids from the *Lymnaea* sequence. One had an N-terminal 3× FLAG but was devoid of the C-terminal (His) tag. The two others contained a 1× FLAG tag on the C terminus or N terminus. Restriction sites were also engineered into the coding sequence at convenient locations to allow for formation of removable cassettes for subsequent mutagenesis studies.

[1]The abbreviations used are: AChBP, acetylcholine-binding protein; *A*-AChBP, *Aplysia* acetylcholine-binding protein; *L*-AChBP, *Lymnaea* acetylcholine-binding protein; nAChR, nicotinic acetylcholine receptor.

Conditions for protein expression paralleled that of the *Lymnaea* AChBP (11). Briefly, HEK cells were transfected with *A*-AChBP cDNA along with a companion neomycin acetyltransferase gene and selected for stable expression using G418. Medium containing the secreted *A*-AChBP was collected at 2–3-day intervals, and cells were replenished with fresh medium. Collected medium was preserved prior to purification with 0.02% NaN_3. *A*-AChBPs were purified by adsorption onto a FLAG antibody column followed by elution with the 3× FLAG peptide.

Fast Protein Liquid Chromatography

Gel filtration was carried out using an Amersham Biosciences LCC 500 plus fast protein liquid chromatograph with a Superdex 200 gel filtration column. Fifty μl of *A*-AChBP protein at a 100 μg/ml protein concentration in Tris-HCl-buffered saline (20 mM Tris-HCl, 150 mM NaCl, pH 7.4) plus 0.02% azide was loaded on the column at a rate of 0.5 ml/min. Protein in the eluent was monitored by absorption at 280 nm.

Sedimentation Equilibrium Analysis

Analytical ultracentrifugation was conducted in a Beckman/Coulter XL-I centrifuge equipped with UV absorption optics using a 60 Ti rotor. Protein solutions of 100 μg/ml were used in a six-channel charcoal-filled epon centerpiece loaded with 110 μl of sample and 125 μl of reference buffer (20 mM Tris-HCl, 150 mM NaCl, pH 7.4). Individual samples were centrifuged at 20 °C for 16 h at 10,000 and 12,000 rpm. Equilibrium was attained as judged by overlay of the last three sequential scans. Data were recorded in step mode with a Δr of 0.001 cm, and five replicate absorption measurements were performed at each step every 2 h. A partial specific volume, $\bar{\nu} = 0.71$, for AChBPs was calculated using Sednterp software (version 1.06), accounting for total sugar composition. Molar masses of the proteins were calculated using XL-A/XL-I data analysis software version 4.0 based on the Origin™ program.

Estimation of Binding Parameters from Fluorescence Signals

Equilibrium fluorescence was monitored using a Tecan Safire fluorescence plate reader (Tecan) in 96-well UV plates (Costar). AChBP was excited at 280 nm, and emission intensity was monitored at 340 nm using an excitation and emission slit widths of 7.5 nm in a bottom read mode at room temperature.

AChBP, 50–100 nM in binding site concentration, was equilibrated with half-log dilutions of ligand. Data were normalized, and K_i values were calculated by fitting to a sigmoidal dose-response curve with variable slope in Prism GraphPad 3.0. Y = minimum + (maximum − minimum)/$(1 + 10^{((\log EC50 - X)*\text{Hill slope})})$, where X represents the log of concentration and Y is the fractional binding. K_i is calculated from $Y_{50}/(1 + ([\text{ligand}]/K_d))$.

To determine ligand stoichiometries, AChBP at 400–650 nM in binding sites, estimated from protein concentration, was titrated with sequentially increasing concentrations of epibatidine or methyllycaconitine. The concentration of binding sites greatly exceeded the K_d of the ligand. Accordingly, quenching was essentially linear with concentration until the binding sites were saturated and no further quenching was apparent.

pH Stability of AchBPs

AChBP at a concentration of 0.5 nM binding sites was mixed with 0.1 mg/ml of beads for the PVT copper His_6 tag scintillation proximity assay, according to the manufacturer's recommendations (Amersham Biosciences). The beads were suspended in 0.01 M phosphate/pyrophosphate buffer between pH 5.0 and 11. [^{3}H]Epibatidine at 20 nM was added to the 200-μl reaction and allowed to equilibrate at room temperature at the respective pH for 1 h or the designated time and then read on a Beckman LS 6500 scintillation counter.

Stopped-flow Kinetics

Stopped-flow measurements were obtained using an Applied Photophysics SX.18MV (Leatherhead, UK) stopped-flow spectrofluorometer. AChBP was excited at 280 nm, and emission was monitored above 305 nm using a cut-off filter. Changes in fluorescence emission intensity were fit to a first order equation, and resulting rates were plotted *versus* ligand concentration. Association and dissociation were estimated from the slope and ordinate intercept. In addition, dissociation rate constants were estimated by monitoring the dissociation rate constants of the ligand-AChBP complex by the addition of excess gallamine and following the increase in fluorescence. Sufficient gallamine was used to ensure that the rate was limited by the dissociating ligand rather than the scavenging of free receptor by gallamine.

RESULTS

Expression of the Acetylcholine-binding Protein from the Synthesized Oligonucleotide

Using the published sequence of AChBP from *L. stagnalis*, a blast search of the Entrez Pub Med protein data base yielded a sequence from *A. californica* (*A*-AChBP) that shared 33% amino acid identity with *Lymnaea*. It contained internal sequence features suggesting that it was a soluble binding protein rather than a truncated receptor sequence. Given that *Aplysia* and *Lymnaea* are evolutionarily distant mollusks, we reasoned that *A*-AChBP might be an ortholog with distinct pharmacological properties. Fig. 1 shows an alignment of soluble binding proteins with the N-terminal domains of transmembrane-spanning heteromeric $(\alpha 1)_2\beta\gamma\delta$ nicotinic receptor in muscle and the homomeric α7 neuronal receptor. *A*-AChBP lacks a transmembrane spanning region. Furthermore, the cysteine loop region between residues 127 and 140 (*Aplysia* numbering) is highly conserved among binding proteins but distinct from that of nAChRs, where it is also highly conserved among the receptor molecules. This region is thought to interact and link with the transmembrane domain of the receptor (7, 13) but reveals a hydrophilic surface in the case of the binding proteins.

HEK 293 cells, transfected with the *A*-AChBP gene and selected as stable transfectants, secreted the encoded protein into the media. Typically between 1 and 3 mg of *A*-AChBP could be purified from a liter of medium. A cDNA encoding *A*-AChBP, isolated from a sensory cell *Aplysia* library, when placed in our viral expression vector, was found not to express active secreted protein. When sequenced, it was found to differ by valine being substituted to alanine at residues 43 and 138. A sequence with the two valine residue substitutions was not found in the *Aplysia* data base.

Characterization of the Binding Protein

Due to variable aggregation of initial preparations of *A*-AChBP, we investigated the role played by a C-terminal His_6 tag and several FLAG tags of variable length at both the N and C termini of the AChBP coding sequence (Fig. 2). Table I shows the typical expression achieved after purification for four constructs for both *Lymnaea* and *Aplysia* genes. Purified protein for each construct was analyzed by SDS-PAGE and gel filtration. A His_6 tag on the C terminus resulted in extensive aggregation or oligomerization in the *Aplysia* cDNA following purification. The aggregation varied from a small shoulder slightly larger than the pentameric 190 kDa to an aggregate peak in the void volume upon gel filtration (Fig. 3, *C* and *D*). The presence of the larger oligomers accumulated rapidly at room temperature and 4 °C. By contrast, the *Lymnaea* protein showed minimal aggregation initially but formed higher order oligomers over a period of several months when stored at 4 °C. Expression from constructs encoding both *Lymnaea* and *Aplysia* protein without the His_6 tag yielded minimal aggregation over several months (Fig. 3, *A* and *B*). Both eluted at an apparent molecular weight of 190,000.

Constructs modified at the N terminus showed variable glycosylation evident in the multiple bands on SDS-PAGE (Fig. 4). Only the construct with a single C-terminal FLAG tag (III) migrated as a single but broad band. Its expression yields, however, were lower than those of the N-terminally tagged constructs (Table I). Neither initial aggregation nor heavy glycosylation was observed to influence ligand binding parameters, although the aggregated proteins were not studied in detail. Analytical ultracentrifugation yielded profiles that fit to a molecular weight estimate of 155,100 ± 1,400 for *A*-AChBP and 151,700 ± 800 for *L*-AChBP (Fig. 5), values expected for a glycosylated pentamer.

We examined protein stability in 0.05 M phosphate/pyrophosphate buffer between pH 5.0 and 11 (Fig. 6). In addition, solutions were kept at room temperature in the dark and stability monitored over a month (data not shown). [^{3}H]Epibatidine sites were not lost during the 1-h incubation for *L*-AChBP between pH 5.5 and 11, whereas *A*-AChBP rapidly lost activity above pH 10. Above pH 8, *L*-AChBP was stable for 6 days but showed some loss of signal after 1 month. *A*-AChBP showed little binding above pH 8.0 after 6 days but was completely stable between pH 6.0 and 7.0 for the observed period.

Ligand Binding Properties

To determine ligand recognition properties of A-AChBP, we employed an equilibrium-binding assay using intrinsic tryptophan fluorescence of AChBPs. Fig. 7 shows typical mass action curves of both *L*-AChBP and *A*-AChBP. Surprisingly, whereas only gallamine was found to enhance tryptophan fluorescence for *L*-AChBP, small cholinergic agonists such as choline, acetylcholine, and carbachol enhanced fluorescence emission of *A*-AChBP in addition to gallamine. Agonists, such as nicotine and epibatidine, containing ring nitrogens markedly quenched fluorescence of both AChBPs.

Binding of ligands with K_d values below 100 nM was monitored using stopped-flow spectrometry and fluorescence detection (see Table III). Table II shows a summary of dissociation constants determined from tryptophan fluorescence either by equilibrium

titration for lower affinity ligands or by kinetic analysis for the high affinity ligands. Interestingly, α-bungarotoxin has 100-fold lower affinity for *A*-AChBP than *L*-AChBP, but the smaller peptide, α-conotoxin ImI, has an affinity for *A*-AChBP that is more than 4 orders of magnitude greater than that for *L*-AChBP. Higher affinity of α-conotoxin ImI for *Aplysia* arises primarily from its slower dissociation rate (Table III). The slow binding, high affinity ligands appear to show a second unimolecular phase of low amplitude for tryptophan fluorescence quenching. This is being investigated in relation to overall mechanism. We reported previously *L*-AChBP to have five binding sites per pentamer (11). Equilibrium titrations of *A*-AChBP at concentrations above its K_d value likewise reveal five sites per pentamer (Fig. 8). Titration profiles are very similar to those reported for the *L*-AChBP.

DISCUSSION

The discovery of an acetylcholine binding protein from the fresh water mollusk *L. stagnalis* and the elucidation of its structure by x-ray crystallography have added a new dimension to the study of the structure and ligand binding properties of the family of nicotinic acetylcholine receptors and related pentameric ligand-gated ion channels (9). Moreover, linking structural details of the extracellular domain from crystallography at 2.8-Å resolution to electron microscopy reconstruction analysis of the transmembrane domain of the nAChR at 4 Å has yielded a more comprehensive structural perspective of the nicotinic receptor as an integral unit (2, 7–9).

The multiplicity of the family of nicotinic receptor subunits and the diversity of subtypes that can be achieved through subunit assembly allow one to rank order selective ligands with respect to receptor subtype. The very size of the nAChR family exceeds the discrimination capacity of its ligands, precluding a receptor subtype classification based solely on ligand specificity. Nevertheless, ligand selectivity of receptor subtypes does allow studies of subtype distribution in regional tissue areas and during developmental processes (14). Developing a complement of AChBPs with distinct specificities would enable one to add a structural dimension to the analysis of the determinants of ligand specificity, since the soluble proteins and their complexes can be analyzed in far more structural detail.

To this end, we have synthesized a cDNA encoding an AChBP from *A. californica* and demonstrated that it assembles as a pentamer, has a stoichiometry of one ligand binding site per subunit or five per pentamer, and exhibits a general profile of ligand binding affinities characteristic of the nAChR. The capacity of the expressed *Aplysia* subunit to assemble as a stable pentamer has been compared with *Lymnaea*. Moreover, we have identified a signature ligand for the *Aplysia* AChBP ortholog where α-conotoxin ImI has 16,000-fold greater affinity for *Aplysia* over the *Lymnaea* protein. Other naturally occurring ligands of peptidic or alkaloid composition also show preferential affinities for the one or the other AChBPs. α-Conotoxin ImI is produced by *Conus imperialis*, a worm-hunting cone snail (15). This conotoxin is known to be a selective ligand for the α7 subtype among the nAChRs (16), suggesting the possibility that ligand specificity of the *Aplysia* AChBP more closely mimics the α7 receptor subtype than *Lymnaea*. Since the *Aplysia* and *Lymnaea* AChBPs only show 26 and 24% amino acid residue identity with the extracellular region of α7, neither binding protein would be a precise replicate homomeric mammalian receptor. However, they present

a potential structural template for substitution of mammalian residue determinants of specificity.

Synthesis, Assembly, and Stability of the Acetycholine-binding Protein

Using a mammalian expression system and cDNAs constructed from oligonucleotides designed to introduce restriction sites at strategic locations and weighted toward a mammalian codon abundance gives rise to expression and export of AChBP into the culture medium in quantities of several milligrams per liter. To increase the surface area of attached cells, we have employed multilayer 100-cm^2 flasks, but the expression system should be applicable to other adhesion attachments for cell growth. Multiple medium changes and replenishment allow for continuous production from single plating for up to a month.

As might be anticipated, expression levels of protein differ substantially between experimental constructs depending on the nature of the recognition tag and where it is placed on the construct. We have employed a FLAG epitope for purification and a His tag for both purification and development of a radioactive assay for the soluble protein. Expression can be achieved with both tags, but stability of the protein and the extent of glycosylation processing differ as evidenced by migration on SDS-PAGE. The products of the expression constructs also differ in their capacity to assemble as pentamers as evidenced by size exclusion chromatography and sedimentation analysis. We routinely examine our preparations to ensure that they are virtually devoid of monomeric species and higher orders of assembly or aggregates prior to analyzing binding parameters.

Both AChBPs can be purified in quantities of several mg, offering the potential for physical investigations of their overall structure in relation to their ligand recognition properties. The purified proteins appear to be quite robust and retain their assembled structure and ligand binding properties for extended periods of time. Of the two, the *Lymnaea* protein appears to assemble more facilely under the many conditions employed and exhibit the greater stability as measured at extreme pH values. The extent of glycosylation appears dependent on the placement of the recognition tag for purification. Glycosylation also appears to be an important factor in the ease of crystallization of the two binding proteins.[2]

Determinants of Ligand Specificity

Since the pioneering findings of Silman and Karlin (17), who demonstrated the importance of vicinal cysteines, now identified in the β_9–β_{10} linker, in the recognition characteristics of the nAChR, elucidating the determinants of recognition for the receptor for the variety of natural and synthetic ligands has become a major endeavor. Studies with site-directed irreversible inhibitors, chemical cross-linking, and site-directed mutagenesis all have identified three noncontiguous segments on the face of the α-subunit and four on the opposing face of the adjacent subunit of the circular pentamer that harbor the side chain determinants governing ligand specificity (18, 19). Identification of these regions and delineation of the characteristics of the residues involved has benefited greatly from the comparison of specificity of homologous subunits, generation of subunit chimeras, and site-

[2]S. B. Hansen, unpublished observations.

directed residue substitutions from the homologous or orthologous subunits (18). This approach is now possible with residue substitutions in the homomeric *Lymnaea* and *Aplysia* pair.

The rate constants for association of α-bungarotoxin are far slower than the other ligands, suggesting that initial binding of this toxin induces a slow change in conformation or the α-toxin binds to a conformation of low abundance. The uniquely slow rates of α-toxin association with the receptor have been known for many years (20, 21). For both α-conotoxin ImI and α-bungarotoxin, differences in affinity for the two AChBPs are reflected primarily in the dissociation rates.

The two AChBPs also differ in several other properties that bear further experimental investigation. For example, the *Aplysia* protein has three tryptophans, whereas *Lymnaea* contains an additional tryptophan at position 53 (corresponding to 55 in *Aplysia*). This is a region in the muscle receptor shown to govern ligand specificity differences seen between the respective binding sites at the αγ, the αε, and the αδ subunit interfaces (18, 19). Given the steric requirements for placement of a large indole ethyl side chain, tryptophan at this position becomes a candidate determinant of the distinct affinities found between the *Aplysia* and the *Lymnaea* AChBPs. Moreover, we have shown previously that many ligands quench the tryptophan fluorescence of the *Lymnaea* protein upon binding; these signals might be exploited further to monitor binding kinetics and ascertain binding orientation of the ligands.

Acknowledgments

We are grateful to Dr. Kelsey Martin at UCLA for providing a sensory cell cDNA library from *A. californica*.

REFERENCES

1. Corringer PJ, Le Novere N, Changeux JP. Annu. Rev. Pharmacol. Toxicol. 2000; 40:431–458. [PubMed: 10836143]
2. Karlin A. Nat. Rev. Neurosci. 2002; 3:102–114. [PubMed: 11836518]
3. Sixma TK, Smit AB. Annu. Rev. Biophys. Biomol. Struct. 2003; 32:311–334. [PubMed: 12695308]
4. Chang CC, Lee CY. Arch. Int. Pharmacodyn. Ther. 1963; 144:241–257. [PubMed: 14043649]
5. Lee CY. Showa Igakkai Zasshi. 1963; 23:221–229. [PubMed: 14083261]
6. Changeux JP, Kasai M, Lee CY. Proc. Natl. Acad. Sci. U. S. A. 1970; 67:1241–1247. [PubMed: 5274453]
7. Kash TL, Jenkins A, Kelley JC, Trudell JR, Harrison NL. Nature. 2003; 421:272–275. [PubMed: 12529644]
8. Miyazawa A, Fujiyoshi Y, Unwin N. Nature. 2003; 424:949–955. [PubMed: 12827192]
9. Brejc K, van Dijk WJ, Klaassen RV, Schuurmans M, van Der Oost J, Smit AB, Sixma TK. Nature. 2001; 411:269–276. [PubMed: 11357122]
10. Smit AB, Syed NI, Schaap D, van Minnen J, Klumperman J, Kits KS, Lodder H, van der Schors RC, van Elk R, Sorgedrager B, Brejc K, Sixma TK, Geraerts WP. Nature. 2001; 411:261–268. [PubMed: 11357121]
11. Hansen SB, Radic Z, Talley TT, Molles BE, Deerinck T, Tsigelny I, Taylor P. J. Biol. Chem. 2002; 277:41299–41302. [PubMed: 12235129]
12. Nielsen H, Engelbrecht J, Brunak S, von Heijne G. Protein Eng. 1997; 10:1–6. [PubMed: 9051728]

13. Unwin N, Miyazawa A, Li J, Fujiyoshi Y. J. Mol. Biol. 2002; 319:1165–1176. [PubMed: 12079355]
14. Zoli, M. Handbook of Experimental Pharmacology. Clementi, FFD.; Gotti, C., editors. Vol. 144. Berlin: Springer-Verlag; 2000. p. 213-246.
15. McIntosh JM, Santos AD, Olivera BM. Annu. Rev. Biochem. 1999; 68:59–88. [PubMed: 10872444]
16. Johnson DS, Martinez J, Elgoyhen AB, Heinemann SF, McIntosh JM. Mol. Pharmacol. 1995; 48:194–199. [PubMed: 7651351]
17. Silman I, Karlin A. Science. 1969; 164:1420–1421. [PubMed: 5783718]
18. Taylor, P. Handbook of Experimental Pharmacology. Clementi, FFD.; Gotti, C., editors. Vol. 144. Berlin: Springer-Verlag; 2000. p. 79-100.
19. Sine SM. J. Neurobiol. 2002; 53:431–446. [PubMed: 12436411]
20. Lee CY. Annu. Rev. Pharmacol. 1972; 12:265–286. [PubMed: 4339019]
21. Weiland G, Georgia B, Lappi S, Chignell CF, Taylor P. J. Biol. Chem. 1977; 252:7648–7656. [PubMed: 914831]
22. Smit, AB.; Sixma, TK. International Patent. WO 01/58951 A2. 2001 Aug 16.

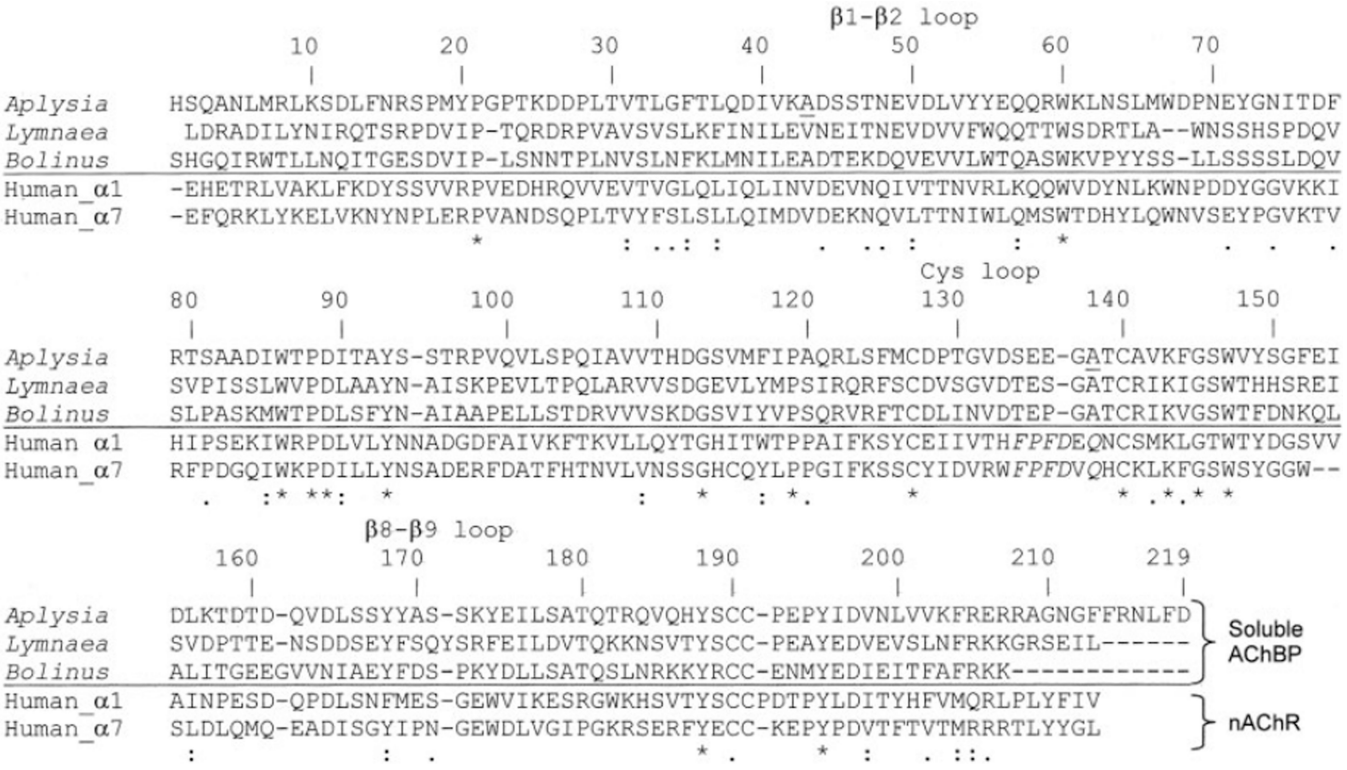

Fig. 1. Protein sequence alignment

Three soluble binding proteins from *L. stagnalis*, *A. californica*, and *Bolinus truncatus* (22) are aligned with the first 210 amino acid residues of human nicotinic acetylcholine receptor α1 and α7 subunits. The numbering corresponds to *Aplysia*, beginning with the first synthesized residue in the cDNA sequence and a probable start site based on consensus sequences. The *asterisks* indicate identity among the receptor family, whereas *colons* and *periods* indicate limited conservation in the series. Underscored alanines 43 and 138 were found to be valines in a sensory cell *Aplysia* cDNA library.

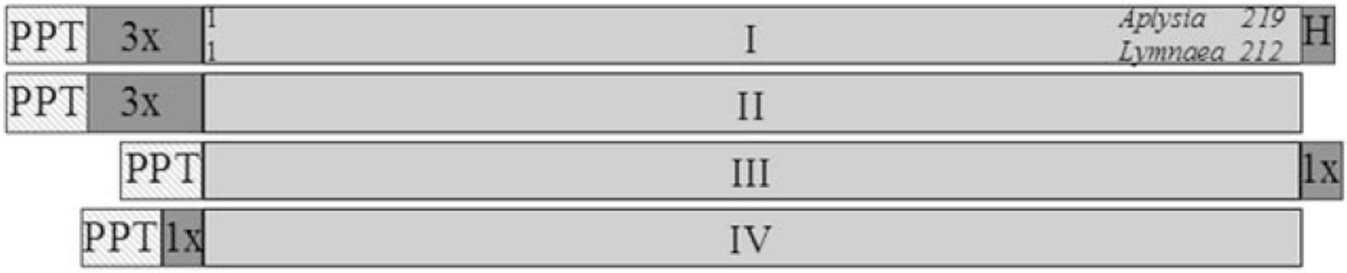

Fig. 2. AChBP cDNA constructs used to characterize the acetylcholine binding protein

PPT, a preprotrypsin leader peptide. *Dark shading* indicates a purification tag (*3*× or *1*×, FLAG epitope; *H*, 6× histidine). Equivalent constructs were made with both *Aplysia* and *Lymnaea*. The *numbers* indicate the respective amino acid residues in the assembled gene products coming from the sequences in Fig. 1.

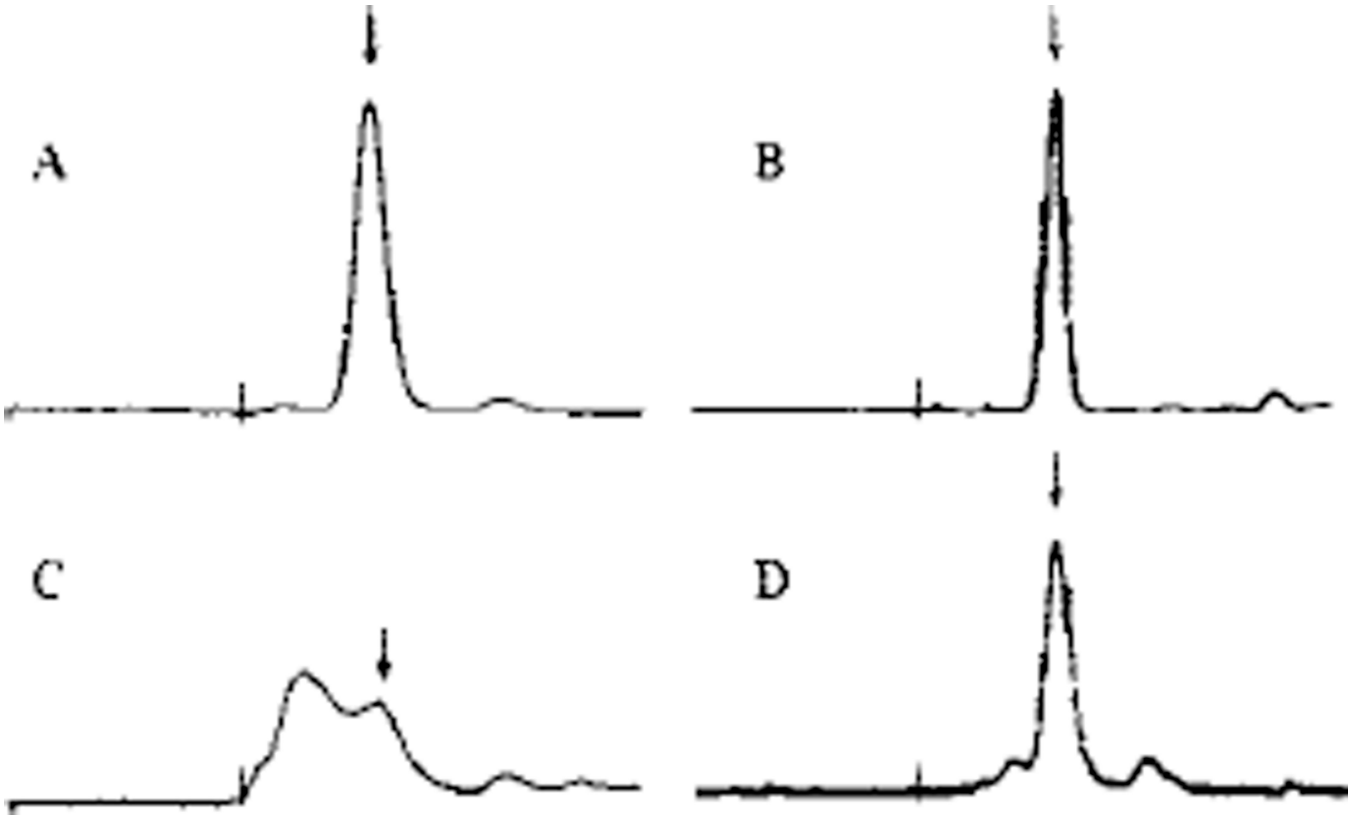

Fig. 3. Fast protein liquid chromatography of AChBPs

A, non-His-tagged A-AChBP (*II*); *B*, non-His-tagged L-AChBP (*II*); *C* and *D*, His-tagged A-AChBP (*I*). The *Roman numerals* designate the constructs in Fig. 2. *C*, ~50% aggregated protein; *D*, mostly properly assembled pentamer with a small shoulder of aggregate. The *arrows* indicate an apparentM_r 190,000 pentamer peak, and *vertical lines* indicate the void volume. Purified AChBP (0.1 mg/ml) in 20 mM Tris-HCl, 150 mM NaCl, pH 7.4, was applied to a Superdex 200 size exclusion column.

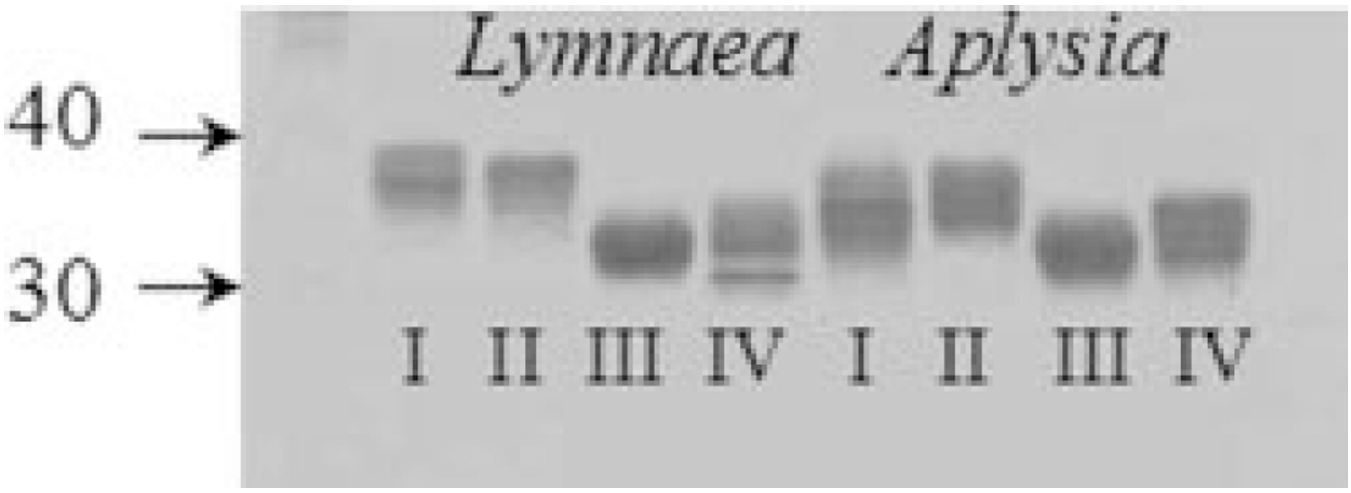

Fig. 4. SDS-PAGE electrophoresis of the purified acetylcholine-binding proteins

Lanes 1–4, Lymnaea proteins; *lanes 5–8, Aplysia* proteins. Size and glycosylation are distinct among tags and seem roughly similar between species. Purified protein (1.5 μg) was spotted on each *lane* and run on 16% acrylamide gels. The *Roman numerals* denote the constructs described in the legend to Fig. 2.

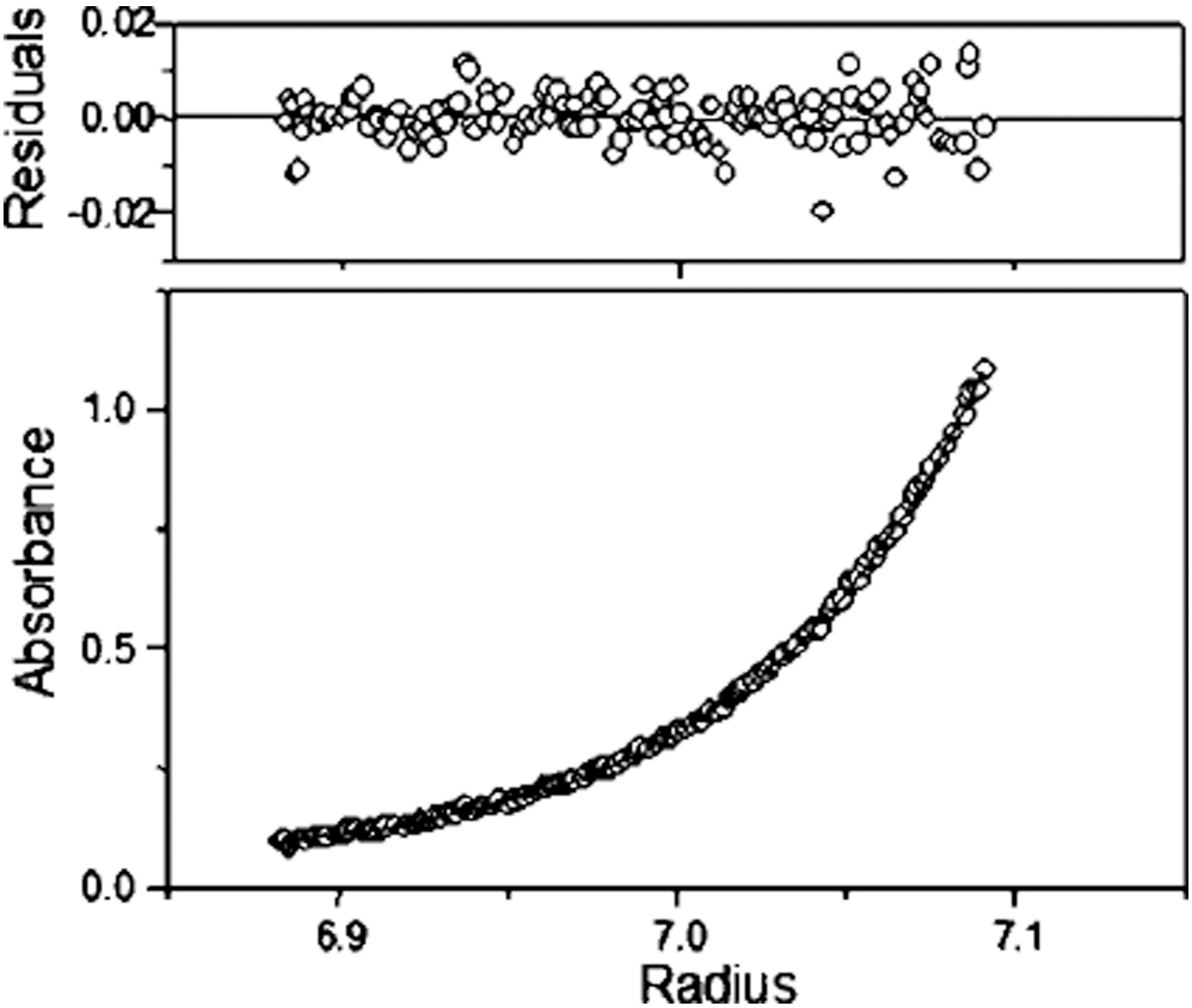

Fig. 5. Analytical ultracentrifugation of *Aplysia* AChBP

Samples of 100 μg/ml A-AChBP in (20 mM Tris-HCl, 150 mM NaCl, pH 7.4) was sedimented at 12,000 rpm until a constant profile was established. The curve is fit to a molecular weight of 153,000 with the other variables fixed as described under "Materials and Methods."

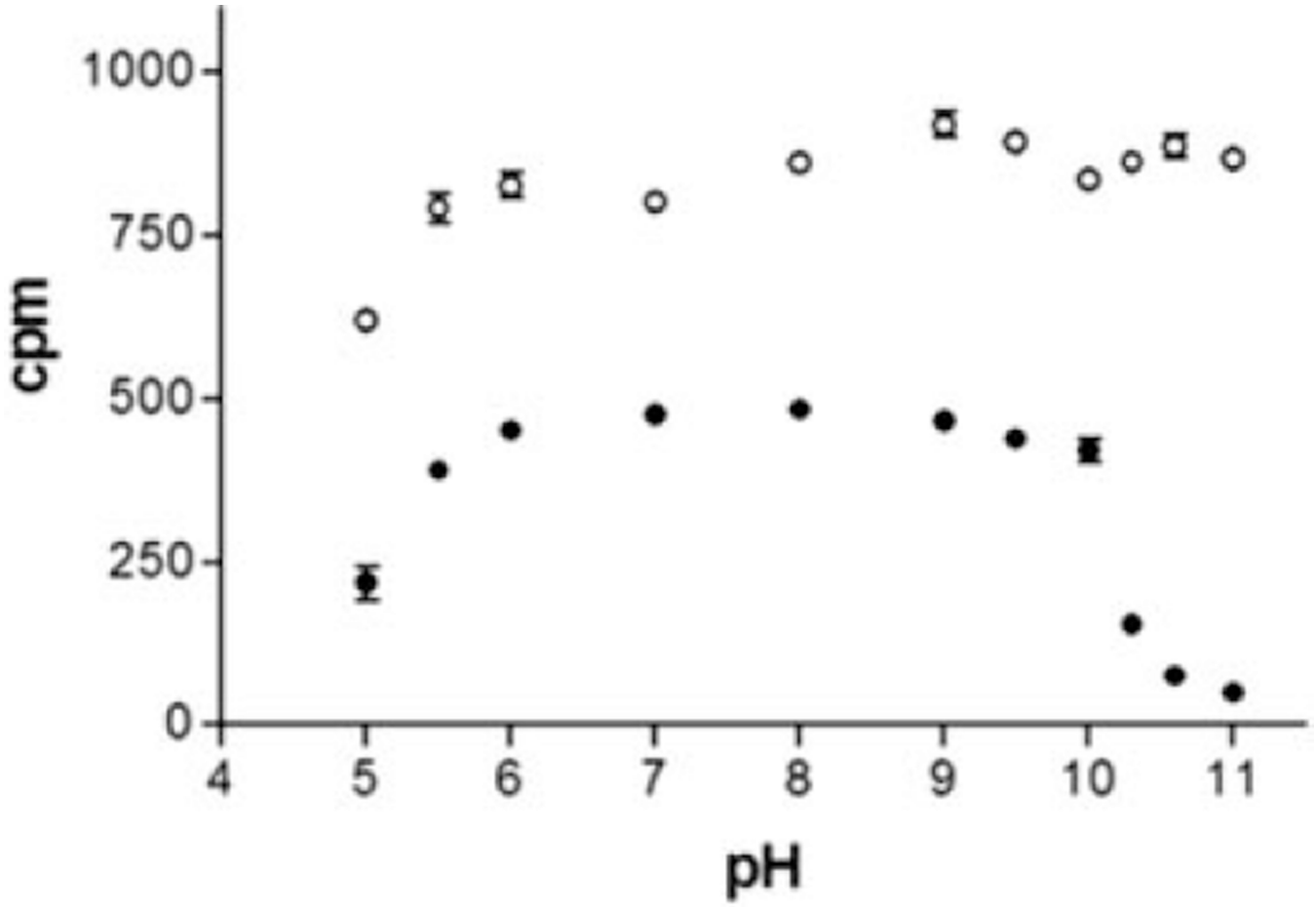

Fig. 6. pH Stability of the AChBPs

Samples of 0.5 nM AChBP binding sites were incubated with 20 nM [^{3}H]epibatidine for 1 h and monitored using a scintillation proximity assay. The pH was varied between 5.0 and 11 using a 100 mM phosphate/pyrophosphate buffer. ○, *L*-AChBP; ●, *A*-AChBP.

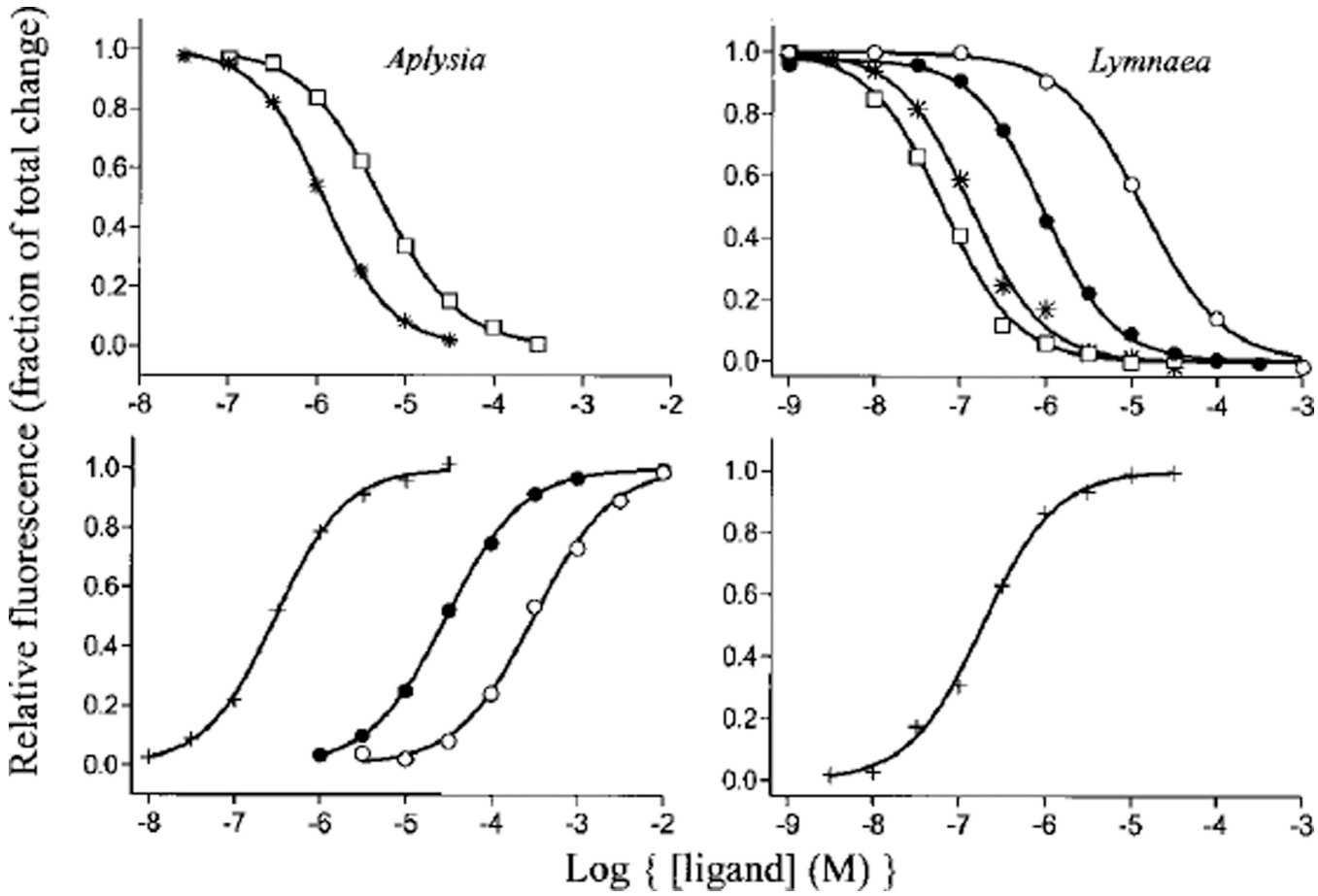

Fig. 7. Equilibrium ligand binding to AChBPs

Ligand binding was monitored in a 96-well fluorescent plate reader. Samples were excited at 280 nm, and intrinsic tryptophan fluorescence was emission-monitored at 340 nm. ○, carbachol; ●, acetylcholine; +, gallamine; *, dansylcholine C_6; □, nicotine). Dissociation constants from experiments such as this are shown in Table II. *Left panels*, *Aplysia* AChBP; *right panels*, *Lymnaea* AChBP.

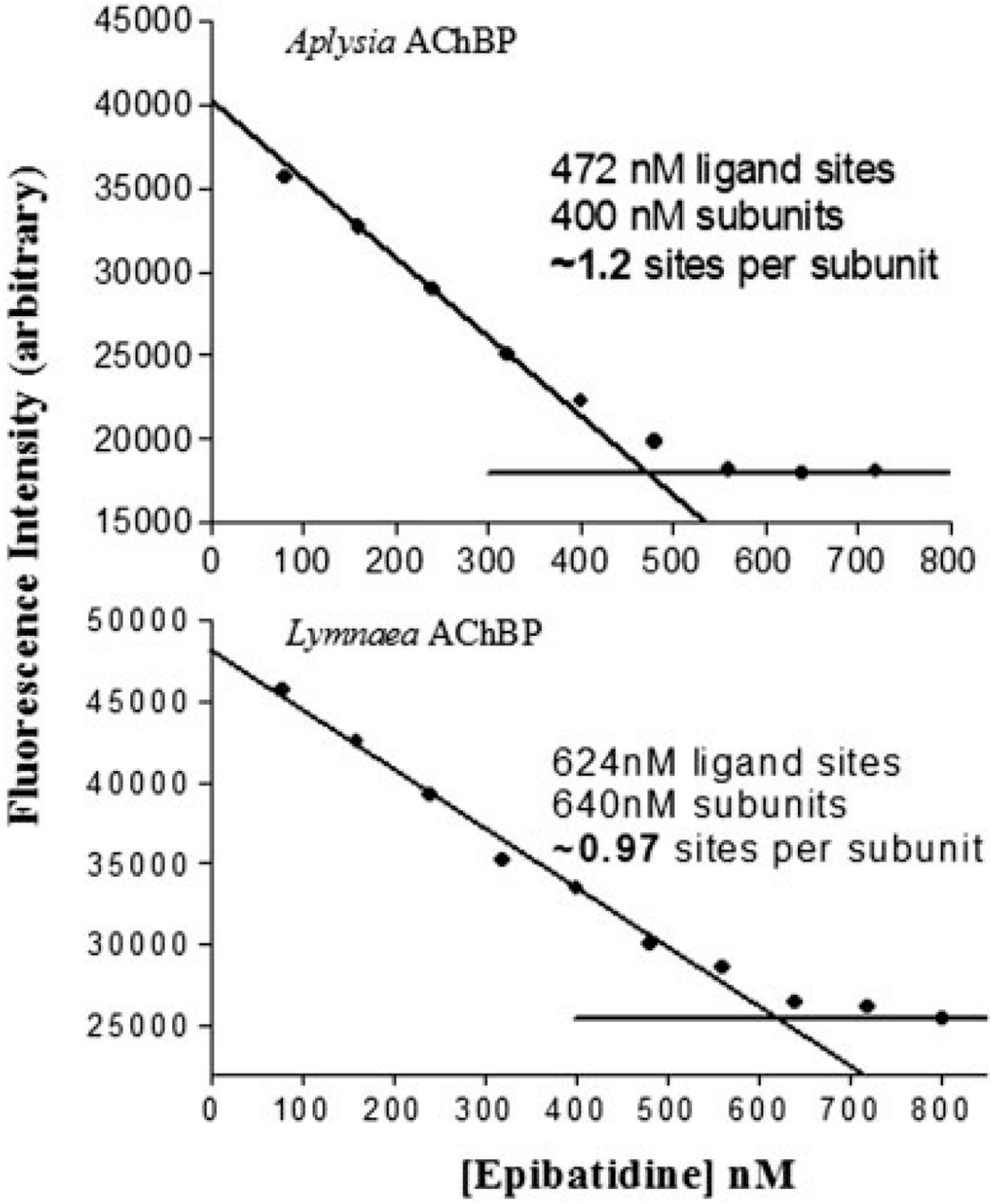

Fig. 8. Titration of ligand stoichiometry

Using excess ligand binding sites over K_d and monitoring intrinsic tryptophan fluorescence quenching of AChBP at 340 nm, binding site titration with [^{3}H]epibatidine was used to estimate the total number of binding sites. Saturation occurs at ~5 sites/pentamer. *Top*, *Aplysia* AChBP; *bottom*, *Lymnaea* AChBP.

TABLE I

Properties of the acetylcholine-binding proteins from Lymnaea and Aplysia

Summarized are the constructs with their corresponding purification tag, molecular weight, expression, and physical properties.

Construct	Peptide M_r[a] (*Lymnaea*)	Peptide M_r (*Aplysia*)	Location of purification tags	Aggregation[b]		Oligosaccharide[c]	Yield[d]
				Aplysia	*Lymnaea*		
							mg/liter
I	27,586	28,941	3 × N-FLAG/C-His_6	+	+/−	+	2–3
II	26,551	27,905	3 × N-FLAG	−	−	+	2–3
III	24,834	26,074	1 × C-FLAG	−	−	−	0.5–1
IV	24,834	26,187	1 × N-FLAG	−	−	+	3–4

[a] Molecular weights designate calculated values for the mature peptide only.

[b] Large additional peaks at heavier apparent molecular weights, as observed by gel filtration, were interpreted as aggregation.

[c] Positive for oligosaccharide indicates extensive glycosylation processing with multiple bands; all forms contain *N*-linked oligosaccharides.

[d] Expression is shown as a range from several preparations, quantified as mg of protein purified to apparent homogeneity/liter of harvested medium.

TABLE II

Dissociation constants for ligand binding to the Aplysia and Lymnaea acetylcholine-binding proteins

Ligand	*Aplysia* K_d	*Lymnaea* K_d	K_d ratio *L/A*
	nM	nM	
α-Conotoxin ImI	0.88[a]	14,000[a]	16,000
Methyllycaconitine	2.8[a]	0.41[b]	0.14
Epibatidine	14[a]	0.16[b]	0.011
Strychnine	15[a]	23[a]	1.5
Gallamine	120[c]	140[b]	1.2
(−)-Nicotine	245[c]	86[b]	0.35
α-Bungarotoxin	250[c]	1.8[b]	0.0071
Dansylcholine C_6[d]	1,600[c]	110[b]	0.069
Acetylcholine	33,000[c]	890[c]	0.027
Carbachol	240,000[c]	5,600[c]	0.023

[a] K_d values for high affinity ligands (K_d values of <100 nM) were determined from the ratio of association and dissociation rates by monitoring intrinsic tryptophan quenching with stopped-flow spectrofluorimetry.

[b] Previously reported in Ref. 11.

[c] Low affinity ligands were measured using equilibrium fluorescence quenching in a 96-well fluorescent plate reader. All constants are either an average of two values or the mean of three or more. Values varied by less than 20%.

[d] 5-Dimethylaminonaphthylsulfonamidohexyltrimethylammonium.

TABLE III

Kinetic constants for association (k_1) and dissociation (k_{-1}) of various ligands for the acetylcholine-binding proteins

Kinetic constants were determined using stopped-flow spectrofluorimetry. Samples were excited with 280-nm light, and emission was monitored above 305 nm. Slow dissociation rates of high affinity ligands were measured by competition. The addition of gallamine induces an enhancement of fluorescence in formation of its complex. Data are averages of two measurements or means of three or more measurements.

Ligand	k_1		k_{-1}	
	Aplysia	*Lymnaea*	*Aplysia*	*Lymnaea*
	$\times 10^8\ M^{-1}\ s^{-1}$		s^{-1}	
α-Conotoxin ImI	0.16	0.014	0.01	19
Epibatidine	2.5	1.7	3.4	0.027
Strychnine	3.0	0.93	4.6	2.2
Methyllycaconitine	0.44	0.13	0.12	0.005
Gallamine	2.5	2.5	65	36
α-Bungarotoxin	0.010	0.009	0.32	0.001
(−)-Nicotine	2.3	1.5	49	5.7